Composite Higgs model at a conformal fixed point

R. C. Brower,[1] A. Hasenfratz,[2] C. Rebbi,[1] E. Weinberg,[1] and O. Witzel[3]

[1]*Department of Physics and Center for Computational Science, Boston University, Boston, Massachusetts 02215, USA*

[2]*Department of Physics, University of Colorado, Boulder, Colorado 80309, USA*

[3]*Higgs Centre for Theoretical Physics, School of Physics & Astronomy, The University of Edinburgh, Edinburgh EH9 3FD, United Kingdom*

(Received 15 December 2015; published 20 April 2016)

We propose to construct a chirally broken model based on the infrared fixed point of a conformal system by raising the mass of some flavors while keeping the others massless. In the infrared limit, the massive fermions decouple, and the massless fermions break chiral symmetry. The running coupling of this system "walks," and the energy range of walking can be tuned by the mass of the heavy flavors. Renormalization group considerations predict that the spectrum of such a system shows hyperscaling. We have studied a model with four light and eight heavy flavors coupled to $SU(3)$ gauge fields and verified the above expectations. We determined the mass of several hadronic states and found that some of them are in the 2–3 TeV range if the scale is set by the pseudoscalar decay constant $F_\pi \approx 250$ GeV. The 0^{++} scalar state behaves very differently from the other hadronic states. In most of our simulations, it is nearly degenerate with the pion, and we estimate its mass to be less than half of the vector resonance mass.

DOI: 10.1103/PhysRevD.93.075028

I. INTRODUCTION

Electroweak symmetry breaking (EWSB) and the nature of the Higgs boson are central questions of beyond the Standard Model (BSM) investigations. A gauge theory exhibiting spontaneous chiral symmetry breaking (SχSB) may describe EWSB when coupled to the Standard Model. In such a system, three of the massless Goldstone pions become the longitudinal component of the $W^\pm$ and Z bosons, while all other hadronic states appear as experimentally observable excitations in the spectrum. The physical energy scale is set by matching the decay constant of the pseudoscalar (pion) to the *vacuum expectation value* of the EWSB, i.e., $F_\pi \approx 250$ GeV. BSM theories based on this construction are particularly interesting as they predict several resonances around 2–3 TeV, an energy range accessible at the LHC. The lightest vector meson state in our model is close to 2 TeV and could correspond to the recently reported resonance [1]. These theories are based on similar concepts originally introduced in the context of technicolor [2–5]. Phenomenologically viable models must have properties quite different from QCD, suggesting they are likely near the conformal boundary. Recent lattice simulations with many fundamental flavors or with fermions in higher representations have indeed revealed non-QCD-like properties [6–11].

A composite BSM model with two massless fermions generates the required three Goldstone bosons. If the number of fermions is larger than two, as is the case in systems with fundamental flavors near the conformal boundary, the additional massless pseudoscalars have to acquire mass. While the precise mechanism of this could be complicated, for an effective description, one can simply add a mass term to the additional fermion flavors. In a model with N_f fermions, one would keep $N_\ell = 2$ flavors massless and make $N_h = N_f - N_\ell$ fermions massive. That way, the system will have only three massless Goldstone bosons in the infrared limit, yet the additional flavors will have an influence on the spectrum.

When the total number of fermions increases above a critical value, the system crosses the conformal boundary. The infrared properties are now characterized by a nonperturbative infrared fixed point (IRFP). Nevertheless, the construction proposed above works just the same. Lifting the masses of all but $N_\ell = 2$ flavors will lead to SχSB with three massless Goldstone bosons in the infrared limit. The presence of the conformal IRFP influences both the running of the gauge coupling and the spectrum. The idea to give mass to some of the flavors studied was previously discussed in Ref. [12], and a similar construction, though with different phenomenology, has been proposed, e.g., in Refs. [13] and [14].

In this paper, we investigate the properties of such a system, based on the $N_f = 12$ conformal model [15–20]. We lift the masses of $N_h = 8$ fermions (heavy flavors) and keep $N_\ell = 4$ flavors light. This choice is motivated by the lattice action we use in our simulations, but a chirally broken model with four light flavors also has phenomenological relevance. An example is the composite two-Higgs-doublet model of Ref. [21] that assumes four light flavors and the Higgs bosons emerge as pseudo-Goldstone states. More commonly discussed models feature two massless fermions in the chiral limit and thus require simulations with $N_\ell = 2$. Our choice is, however, sufficient to investigate general properties of mass split systems. By changing m_h from zero to ∞, our model interpolates between the conformal 12-flavor and the chirally broken 4-flavor systems. If $m_h > 0$, chiral symmetry is spontaneously broken. In the next section, we deduce that the hadron spectrum of the light flavors shows hyperscaling in m_h assuming m_h is in the scaling regime of the IRFP and $m_\ell = 0$. Ratios of hadron masses are independent of m_h, yet by tuning $m_h \to 0$ one can control the energy dependence of the gauge coupling, making it walking. Walking, in turn, can influence some of the infrared properties important to satisfy electroweak constraints.

We study both the hadron spectrum and the running gauge coupling in numerical simulations and verify theoretical expectations. In particular, we show that ratios of hadron masses in the $m_\ell = 0$ chiral limit are independent of m_h in the scaling regime of the IRFP. We compare the predicted spectrum with QCD and the conformal $N_f = 12$-flavor systems. Despite some similarities, the spectrum we observe is distinct from both QCD and the $N_f = 12$ predictions. Setting the energy scale by $F_\pi \approx 250$ GeV, we predict the lightest vector excitation to be around 2 TeV. The mass of the isomultiplet scalar is only slightly larger, while the nucleon and axial vector are both around 2.7 TeV. At the fermion masses we can investigate, the mass of the isosinglet scalar is comparable to the pion. Thus, predicting its chiral limit value is difficult, and we only quote the bound $M_{0^{++}}/F_\pi \lesssim 4$. Simulations on larger volumes and smaller fermion masses are needed to make this prediction more precise. In addition, when coupled to the SM heavy quarks, radiative corrections will lower the mass of the scalar considerably [22]. Preliminary results of both the spectrum and running coupling were presented in Refs. [23,24], and a publication with further details is in preparation [25].

II. RENORMALIZATION GROUP STRUCTURE AND RUNNING COUPLING

Our 4 + 8-flavor model is built on the conformal IRFP of the SU(3) $N_f = 12$-flavor system. Near the IRFP, the only relevant parameter is the fermion mass. When all fermions have a degenerate mass that is much smaller than the lattice cutoff $\Lambda_a \propto 1/a$, we expect hyperscaling with mass scaling dimension $y_m = 1 + \gamma_m \approx 1.25$ [15,16,19]. The Wilson renormalization group (RG) equations predict that a change in the energy scale $\mu \to \mu' = \mu/b$ $(b > 1)$ transforms the bare mass $\hat{m} = am$ as $\hat{m} \to \hat{m}' = b^{y_m}\hat{m}$, while the bare gauge coupling $g \to g'$ approaches its fixed point value $g_\star$. (For simplicity, we consider only one gauge coupling, ignoring all other irrelevant couplings.) It is straightforward to derive a scaling relation for any two-point correlation function C_H [26,27],

$$C_H(t; g, \hat{m}_i, \mu) = b^{-2y_H} C_H(t/b; g', \hat{m}'_i, \mu), \qquad (1)$$

where y_H denotes the scaling dimensions of operator H. With repeated RG steps, the irrelevant couplings approach the IRFP, and the b dependence of Eq. (1) can be written as $C_H \propto b^{-2y_H} F(t/b, b\hat{m}^{1/y_m})$ where F is some unknown function. Since correlation functions are expected to show an exponential decay $C_H(t) \propto \exp(-M_H t)$ when the fermion mass is finite, Eq. (1) implies the scaling relation

$$aM_H \propto (\hat{m})^{1/y_m}. \qquad (2)$$

The renormalization group equation (1) is valid even when some of the fermions are kept massless [24]. The hyperscaling relation of Eq. (2) remains unchanged with the replacement $\hat{m} \to \hat{m}_h$ and applies for both light and heavy flavored hadrons, as long as $\hat{m}_\ell = 0$ and all heavy flavors are degenerate. Therefore, dimensionless ratios, such as M_H/F_π, are independent of the heavy mass, as long as $\hat{m}_h$ is in the scaling regime of the IRFP. Since this system is chirally broken, even the hadrons made up of light flavors are massive (except the Goldstone pions), and hyperscaling implies that their mass in units of F_π is independent of the heavy flavor mass.

Nevertheless, even for $\hat{m}_h \to 0$, the heavy flavors will influence other observables. Consider, e.g., the running gauge coupling as sketched in the top panel of Fig. 1. At high energies, the coupling runs from the bare coupling toward the IRFP. At the UV energy scale denoted by Λ_{UV}, the gauge coupling reaches the vicinity of the IRFP. Its value is close to $g_\star$ and changes only slowly when further reducing the energy scale. In this regime, the coupling "walks." If all fermions were massless, $g(\mu \to 0) = g_\star$ as is indicated by the solid line in the figure. On the other hand, if some of the fermions are massive, their mass becomes comparable to the cutoff at some energy scale, denoted by Λ_{IR}, and they decouple. In this limit, the system behaves like a chirally broken model with N_ℓ massless fermions. The corresponding fast running coupling is denoted by the dashed blue lines in Fig. 1. The walking range between the scales Λ_{UV} and Λ_{IR} can be tuned by $\hat{m}_h$, and a walking behavior in these systems is guaranteed. The red long-dashed curve in Fig. 1 describes the case where the heavy fermions decouple before the gauge coupling reaches the vicinity of the IRFP. This situation can be avoided by tuning $\hat{m}_h \to 0$ and is not considered here.

Our numerical simulations support the expectations outlined above. The bottom panel of Fig. 1 shows the running coupling calculated at five different values, $\hat{m}_h = 0.050$, 0.060, 0.080, 0.100, and ∞ (i.e., $N_f = 4$). We define the energy dependent running coupling through the Wilson flow scheme and match the scales such that all five systems predict the same $g^2(\mu)$ in the infrared limit [28,29]. The $N_f = 4$ system shows the expected fast running, but a shoulder develops as $\hat{m}_h$ is lowered. The dashed curves in the bottom panel of Fig. 1 indicate regions where cutoff effects could be significant; however,

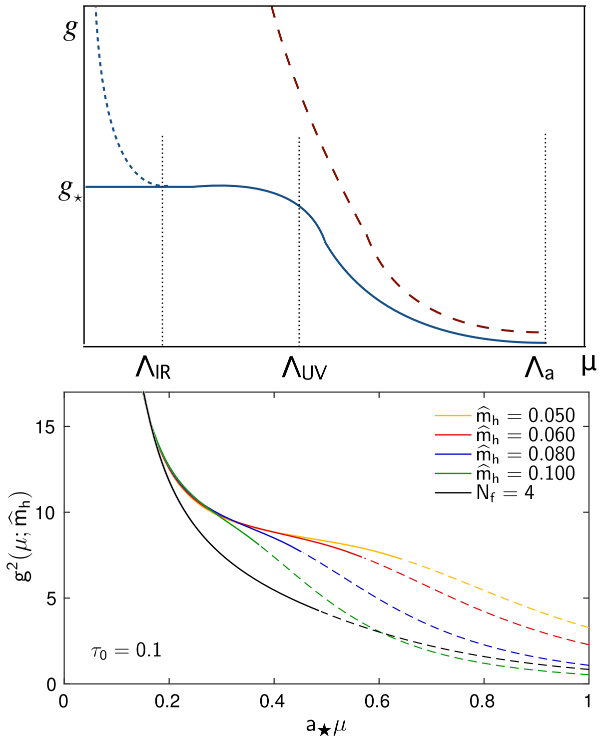

FIG. 1. Top: The expected running gauge coupling of conformal and mass-split systems. The solid blue curve sketches the evolution of the gauge coupling in a conformal system. The dashed blue curve shows the change in a mass-split system, while the red long-dashed curve describes a situation where the fermions decouple before the gauge coupling could approach the conformal IRFP. Bottom: Numerical results for the running coupling constant g^2 for different values of $\hat{m}_h$ and in the $\hat{m}_h = \infty$ (four-flavor limit) with $\hat{m}_\ell$ extrapolated to the chiral limit. The emergence of the walking regime is evident as $\hat{m}_h \to 0$. The dashed sections of the lines indicate where we suspect cutoff effects may be significant.

theoretical considerations guarantee that the gauge coupling takes its IRFP value as $\hat{m}_h \to 0$. The similarity between the top and bottom panels of Fig. 1 is striking and suggests that our simulations have entered the walking regime. A walking gauge coupling leads to the enhancement of the fermion condensate and is necessary to satisfy electroweak constraints.

III. LATTICE SIMULATIONS AND THE HADRON SPECTRUM

Wilson renormalization group considerations predict that the 4 + 8-flavor system shows hyperscaling in the $am_\ell = 0$ chiral limit where dimensionless ratios of hadron masses are independent of the heavy mass am_h. However, these ratios have to match neither the $N_f = 12$- nor the $N_f = 4$-flavor values. In this section, we present numerical results for the hadron spectrum of the $N_f = 4 + 8$ model at four different am_h values.

We use staggered fermions with nHYP smeared gauge links [30,31] and a gauge action that is the combination of fundamental and adjoint plaquette terms. This action has been used in $N_f = 12$-flavor simulations [15,16,19], and we chose the parameters for this work based on those results. We have carried out simulations at one gauge coupling, $\beta = 4.0$, and four different values of the mass of the heavy flavors, $am_h = 0.050$, 0.060, 0.080, and 0.100. Based on the results of the finite size scaling study [19], we expect that the three lightest values are within the scaling regime of the IRFP, while $m_h = 0.100$ could be on the boundary. We chose the light fermion masses in the range $am_\ell = 0.003$–0.035, and the lattice volumes vary from $24^3 \times 48$ to $48^3 \times 96$. At many (am_ℓ, am_h) mass values, we consider two volumes to monitor finite volume effects. We use the Wilson flow transformation to define the lattice scale [28]. As $am_\ell \to 0$ and $am_h \to 0$, our simulations approach the $N_f = 12$ conformal limit, and consequently the lattice spacing decreases, requiring simulations on increasingly larger volumes. Since we observe significant changes in the lattice spacing both when varying am_h and am_ℓ, we present our results in terms of a common reference scale $a_\star$ that we define as the lattice scale on the $(36^3 \times 64$, $am_h = 0.080$, $am_\ell = 0.003)$ ensemble and convert results on other ensembles using ratios of the Wilson flow scale.

Figure 2 summarizes our results of the hadron spectrum. The panels show dimensionless ratios M_H/F_π for the pseudoscalar (pion), vector (rho), isomultiplet scalar (a_0), axial vector (a_1), nucleon (N), and isosinglet scalar (0^{++}) states. The first narrow panel shows the values for QCD [32] which is known to be similar to $N_f = 4$, our $m_h \to \infty$ limit. The last panel presents averages of numerical results for 12 degenerate flavors also accounting for the spread in the literature [7,16,33,34]. (In conformal systems, the ratios are expected to be constant, up to corrections due to scaling violation.) The wider panels in the middle show the $N_f = 4 + 8$ spectrum as the function of the light fermion mass measured in terms of the common lattice scale $a_\star$ at our four am_h values. The errors in Fig. 2 are statistical only. Based on the comparison of different volumes, we estimate that finite volume effects are below the few percent level. We indicate data points by an open symbol where we suspect larger systematic effects. Details will be discussed in Ref. [25].

Since the $N_f = 4 + 8$ system is chirally broken, we expect the pion mass to scale as $M_\pi \propto \sqrt{m_\ell}$, while all other hadrons should acquire finite mass in the $am_\ell = 0$ chiral limit. For large am_h in the limit $am_\ell \to 0$, we observe QCD-like behavior; i.e., M_π/F_π decreases, and M_{a_1}/F_π increases toward the QCD value. On the other hand, our system describes degenerate 12 flavors in the limit of $am_\ell = am_h \ll 1$. At our largest m_ℓ values corresponding to $am_\ell = 0.035$, we find all six ratios to be in agreement with the 12-flavor averages.

The ratios M_H/F_π for the ϱ, a_0, and nucleon states show a fairly linear dependence on $a_\star m_\ell$, allowing for a

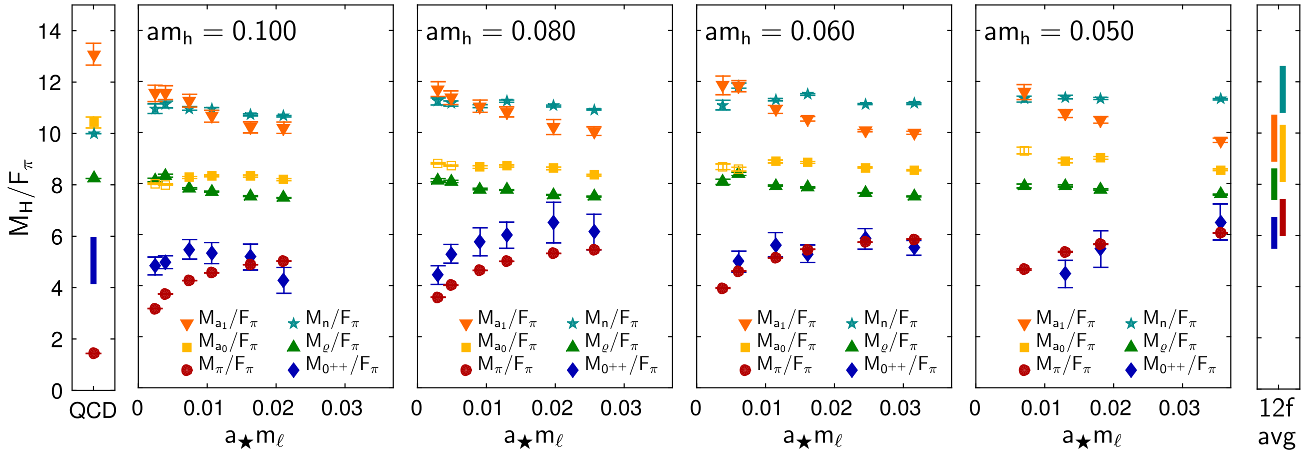

FIG. 2. The pion, rho, isosinglet 0^{++} and isomultiplet a_0 scalar, axial, and nucleon mass of the light flavor spectrum in units of F_π. The first narrow panel shows the experimental values for QCD [32] normalized by $F_\pi = 94$ MeV, while the last one corresponds to average values obtained from $N_f = 12$-flavor simulations [7,16,33,34]. The four wider panels show the $N_f = 4 + 8$ spectrum as the function of the light quark mass $a_\star m_\ell$ for $am_h = 0.100$, 0.080, 0.060, and 0.050. If the chirally broken $N_f = 4 + 8$ system triggered EWSB, $F_\pi \approx 250$ GeV would set the correct electroweak scale.

simple estimate of their values in the $m_\ell = 0$ chiral limit. On the other hand, extrapolating the isosinglet 0^{++} state to the chiral limit is much more difficult. At $am_h = 0.050$ and 0.060, the 0^{++} is degenerate with the pion at all our am_ℓ values, indicating that our light fermions are not light enough to be in the chiral regime. For $am_h = 0.080$ and 0.100, the 0^{++} slowly separates from the pion indicating a nonzero $M_{0^{++}}/F_\pi$ value as $m_\ell \to 0$. This is the expected behavior because the 0^{++} is not a Goldstone boson.

Testing the hyperscaling hypothesis (valid only in the chiral limit), we compare our four different am_h values in Fig. 3. The left panel shows the ratios for the pion, rho, and a_1 exhibiting very little scatter in am_h. In particular, M_ϱ/F_π seems to be independent of the mass of the heavy flavors with a chiral limit of just above 8.0. Thus, the vector state in our model would be around 2 TeV if $F_\pi \approx 250$ GeV. Interestingly, many other near conformal models with an $SU(3)$ gauge group, like the $N_f = 8$ fundamental [11,35], the $N_f = 2$ sextet [36], and even the conformal $N_f = 12$ fundamental [16,33,34], as well as QCD predict almost the same M_ϱ/F_π ratio. Reference [11] argues that this could be a consequence of some remnant vector meson dominance—an idea worth exploring in the future.

The right panel of Fig. 3 shows the ratios for the 0^{++}, a_1, and nucleon. Here, we observe a larger spread for different am_h. At this point, we cannot say whether this spread is due to systematical errors or a possible breakdown of hyperscaling, because corrections to hyperscaling may depend on the observable. In the case of the nucleon, the staggering of the different am_h values might be interpreted to approach the four-flavor QCD-like limit. The a_0 state is more difficult to interpret, since systematic effects are increasing as $m_\ell \to 0$ [25]. The 0^{++} receives contributions from disconnected diagrams, and thus the signal is noisier and

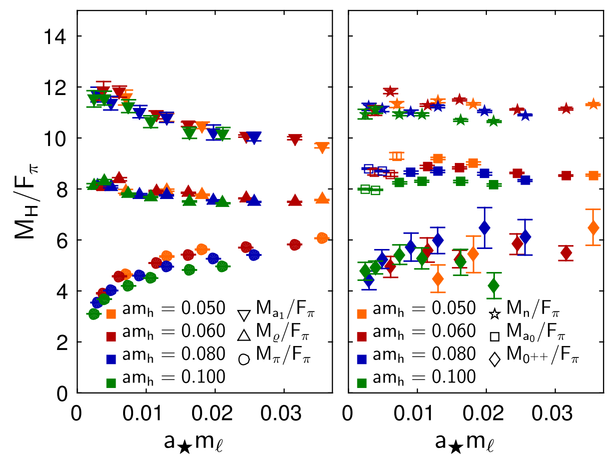

FIG. 3. Combining all four am_h values from Fig. 2. The left panel shows the pion, rho, and a_1, and the right panel shows the 0^{++}, a_0, and nucleon states in units of F_π.

the spread less significant. Overall, the 0^{++} shows a coherent trend: for larger am_ℓ, it is degenerate with the pion—a behavior previously observed in $N_f = 8$ simulations [8,11,37]—and approaches the value of the degenerate 12-flavor limit [7]. When am_ℓ decreases, the 0^{++} becomes lighter, and a linear extrapolation of the data for $a_\star m_\ell \leq 0.01$ would predict a chiral value $M_{0^{++}}/F_\pi \approx 4$. This value is half of the vector resonance and thus lower than the prediction in QCD. However, it is possible that smaller am_ℓ values, especially when m_h is closer to the IRFP, could extrapolate to an even lower mass value.

IV. OUTLOOK AND CONCLUSION

We study a model with spontaneously broken chiral symmetry built on the infrared fixed point of a conformal system by splitting the fermion masses. Specifically, we study a system with $N_\ell = 4$ light (massless) and $N_h = 8$ heavy flavors. Renormalization group arguments imply this system exhibits a walking gauge coupling tunable with the heavy fermion mass and the spectrum shows hyperscaling. Even though our model has four massless fermions in the infrared, its spectrum is not QCD-like. We predict ratios M_H/F_π for several hadronic states. Using the value $F_\pi \approx 250$ GeV, the lightest vector excitation would be around 2 TeV, the mass of the isomultiplet scalar only slightly larger, while the nucleon and axial vector are both around 2.7 TeV. The 0^{++} scalar state remains close to the pion in most of our simulations even when the rho is close to the two-pion threshold, a behavior not observed in QCD simulations. Thus, we expect the 0^{++} to be light, at most half of the vector state. However, since our simulations imply the light fermions are not yet in the chiral regime, it is difficult to predict the mass of the scalar state. In addition, the scalar mass will decrease further due to top-loop corrections when coupled to the SM.

In summary, our model exhibits a light 0^{++} state (Higgs candidate) and predicts additional resonances in the 2–3 TeV range. Most remarkably, the latter predictions seem to be rather universal for BSM models based on the SU(3) gauge theory and are most likely within the reach LHC run II. If the confidence on the 2 TeV resonance [1] increases, further studies are warranted. We are considering simulations of models with only two light flavors that are closer to the conformal window.

ACKNOWLEDGMENTS

The authors thank their colleagues in the LSD Collaboration for fruitful and inspiring discussions. Computations for this work were carried out in part on facilities of the USQCD Collaboration, which are funded by the Office of Science of the U.S. Department of Energy, on computers at the MGHPCC, in part funded by the National Science Foundation, and on computers allocated under the NSF Xsede program to Project No. TG-PHY120002. We thank Boston University, Fermilab, the NSF, and the U.S. DOE for providing the facilities essential for the completion of this work. R. C. B., C. R., and E. W. were supported by DOE Grant No. DE-SC0010025 and in addition acknowledge the support of NSF Grant No. OCI-0749300. A. H. acknowledges support of the DOE Grant No. DE-SC0010005. O. W. is supported by STFC, Grant No. ST/L000458/1. This project has received funding from the European Union's Horizon 2020 research and innovation program under the Marie Skłodowska-Curie Grant No. 659322. R. C. B., A. H., and C. R. thank the Aspen Center for Physics, which is supported by National Science Foundation Grant No. PHY-1066293. R. C. B., A. H., and O. W. thank the KITP, Santa Barbara, supported in part by the National Science Foundation under Grant No. NSF PHY11-25915. A. H. and O. W. thank the CERN Theory group for their hospitality during the completion of this manuscript.

[1] G. Aad *et al.* (ATLAS Collaboration), J. High Energy Phys. 12 (2015) 055; CMS Collaboration, CERN Report No. CMS-PAS-EXO-14-010, 2015.
[2] S. Weinberg, Phys. Rev. D **19**, 1277 (1979).
[3] L. Susskind, Phys. Rev. D **20**, 2619 (1979).
[4] E. Eichten and K. D. Lane, Phys. Lett. **90B**, 125 (1980).
[5] T. Appelquist, J. Terning, and L. C. R. Wijewardhana, Phys. Rev. D **44**, 871 (1991).
[6] F. Bursa, L. Del Debbio, D. Henty, E. Kerrane, B. Lucini, A. Patella, C. Pica, T. Pickup, and A. Rago, Phys. Rev. D **84**, 034506 (2011).
[7] Y. Aoki, T. Aoyama, M. Kurachi, T. Maskawa, K.-i. Nagai, H. Ohki, E. Rinaldi, A. Shibata, K. Yamawaki, and T. Yamazaki (LatKMI Collaboration), Phys. Rev. Lett. **111**, 162001 (2013).
[8] Y. Aoki, T. Aoyama, M. Kurachi, T. Maskawa, K. Miura, K.-i. Nagai, H. Ohki, E. Rinaldi, A. Shibata, K. Yamawaki, and T. Yamazaki (LatKMI Collaboration), Phys. Rev. D **89**, 111502 (2014).
[9] A. Hietanen, R. Lewis, C. Pica, and F. Sannino, J. High Energy Phys. 07 (2014) 116.
[10] Z. Fodor, K. Holland, J. Kuti, S. Mondal, D. Nogradi, and C. H. Wong, *Proc. Sci.* LATTICE2014 (2015) 244.
[11] T. Appelquist *et al.* (LSD Collaboration), arXiv:1601.04027.
[12] D. D. Dietrich and F. Sannino, Phys. Rev. D **75**, 085018 (2007).
[13] L. Vecchi, arXiv:1506.00623.
[14] M. A. Luty and T. Okui, J. High Energy Phys. 09 (2006) 070.
[15] A. Hasenfratz, Phys. Rev. Lett. **108**, 061601 (2012).
[16] A. Cheng, A. Hasenfratz, Y. Liu, G. Petropoulos, and D. Schaich, Phys. Rev. D **90**, 014509 (2014).
[17] A. Cheng, A. Hasenfratz, G. Petropoulos, and D. Schaich, J. High Energy Phys. 07 (2013) 061.
[18] E. Itou and A. Tomiya, *Proc. Sci.* LATTICE2014 (2014) 252.
[19] A. Cheng, A. Hasenfratz, Y. Liu, G. Petropoulos, and D. Schaich, J. High Energy Phys. 05 (2014) 137.
[20] M. P. Lombardo, K. Miura, T. J. N. da Silva, and E. Pallante, J. High Energy Phys. 12 (2014) 183.
[21] T. Ma and G. Cacciapaglia, J. High Energy Phys. 03 (2016) 211.
[22] R. Foadi, M. T. Frandsen, and F. Sannino, Phys. Rev. D **87**, 095001 (2013).

[23] R. C. Brower, A. Hasenfratz, C. Rebbi, E. Weinberg, and O. Witzel, J. Exp. Theor. Phys. **120**, 423 (2015); *Proc. Sci.* LATTICE2014 (2014) 254; E. Weinberg, R. C. Brower, A. Hasenfratz, C. Rebbi, and O. Witzel, J. Phys. Conf. Ser. **640**, 012055 (2015).

[24] A. Hasenfratz, R. C. Brower, C. Rebbi, E. Weinberg, and O. Witzel, arXiv:1510.04635.

[25] R. C. Brower, A. Hasenfratz, C. Rebbi, E. Weinberg, and O. Witzel (unpublished).

[26] T. DeGrand and A. Hasenfratz, Phys. Rev. D **80**, 034506 (2009).

[27] L. Del Debbio and R. Zwicky, Phys. Rev. D **82**, 014502 (2010).

[28] M. Lüscher, J. High Energy Phys. 08 (2010) 071.

[29] A. Hasenfratz, *Proc. Sci.* LATTICE2014 (2015) 257.

[30] A. Hasenfratz and F. Knechtli, Phys. Rev. D **64**, 034504 (2001).

[31] A. Hasenfratz, R. Hoffmann, and S. Schaefer, J. High Energy Phys. 05 (2007) 029.

[32] K. A. Olive *et al.* (Particle Data Group Collaboration), Chin. Phys. C **38**, 090001 (2014).

[33] Y. Aoki, T. Aoyama, M. Kurachi, T. Maskawa, K.-i. Nagai, H. Ohki, A. Shibata, K. Yamawaki, and T. Yamazaki (LatKMI Collaboration), Phys. Rev. D **86**, 054506 (2012).

[34] Z. Fodor, K. Holland, J. Kuti, D. Nogradi, C. Schroeder, K. Holland, J. Kuti, D. Nogradi, and C. Schroeder, Phys. Lett. B **703**, 348 (2011).

[35] Y. Aoki, T. Aoyama, M. Kurachi, T. Maskawa, K.-i. Nagai, H. Ohki, A. Shibata, K. Yamawaki, and T. Yamazaki (LatKMI), Phys. Rev. D **87**, 094511 (2013).

[36] J. Kuti, KITP, Lattice Gauge Theory for the LHC and Beyond, Santa Barbara, CA, 2015 (unpublished).

[37] E. Rinaldi (LSD Collaboration), arXiv:1510.06771; E. Weinberg, 33rd International Symposium on Lattice Gauge Theory, Kobe, Japan, 2015 (unpublished).